PHYSICAL REVIEW FLUIDS **2**, 100505 (2017)

Mechanics of jumping on water

Ho-Young Kim,[1,2,*] Juliette Amauger,[3] Han-Bi Jeong,[1] Duck-Gyu Lee,[4] Eunjin Yang,[5] and Piotr G. Jablonski[6,7]

[1]*Department of Mechanical and Aerospace Engineering, Seoul National University, Seoul 08826, Korea*

[2]*Urban Data Science Lab, SNU BDI, Seoul 06324, Korea*

[3]*Département de Physique, Ecole Normale Supérieure, PSL Research University, 24 rue Lhomond, 75005, Paris, France*

[4]*Department of Nature-Inspired Nanoconvergence Systems, Korea Institute of Machinery and Materials, Daejeon 34103, Korea*

[5]*Korea Institute of Science and Technology Evaluation and Planning, Seoul 06775, Korea*

[6]*School of Biological Sciences, Seoul National University, Seoul 08826, Korea*

[7]*Institute and Museum of Zoology, Polish Academy of Sciences, Wilcza 64, 00-679 Warsaw, Poland*

(Received 16 July 2017; published 17 October 2017)

Some species of semiaquatic arthropods including water striders and springtails can jump from the water surface to avoid sudden dangers like predator attacks. It was reported recently that the jump of medium-sized water striders is a result of surface-tension-dominated interaction of thin cylindrical legs and water, with the leg movement speed nearly optimized to achieve the maximum takeoff velocity. Here we describe the mathematical theories to analyze this exquisite feat of nature by combining the review of existing models for floating and jumping and the introduction of the hitherto neglected capillary forces at the cylinder tips. The theoretically predicted dependence of body height on time is shown to match the observations of the jumps of the water striders and springtails regardless of the length of locomotory appendages. The theoretical framework can be used to understand the design principle of small jumping animals living on water and to develop biomimetic locomotion technology in semiaquatic environments.

DOI: 10.1103/PhysRevFluids.2.100505

I. INTRODUCTION

The locomotion of semiaquatic arthropods, such as water striders, springtails, and fishing spiders, has long fascinated hydrodynamicists as well as biologists for its unique features differentiated from any other large aquatic animals. Their bodies are covered with super-water-repellent hairs [1], which allow them to float on water without effort. Since almost no body parts are immersed in water, their lateral locomotion is described as skating or walking rather than swimming. Living on the air-water interface and having inherently small sizes, they rely on capillary forces, which are important only at or below millimetric scales, for both floatation and propulsion. Some species do not even need to actively move their appendages to propel across the water surface; the gradient of the capillary force generated either by surfactant secretion [2] or meniscus deformation [3] allows small insects or larvae to travel on the water surface.

The focus of this work is on the vertical, rather than lateral, propulsion of the arthrodpods, especially water striders [4] and springtails [5]. Several species of aquatic animals can launch themselves into the air from under the water surface, like copepods [6,7], penguins [8], dolphins [9], and even synchronized swimmers. But they generate thrust for jumping under water using their usual swimming stroke, by undulating their bodies or rowing their appendages. In contrast, the semiaquatic arthropods appear to get airborne without any cumbersome propulsion. As seen in Fig. 1(a), only a single stroke is enough to lift the water strider off the water surface to a height several times the

*hyk@snu.ac.kr

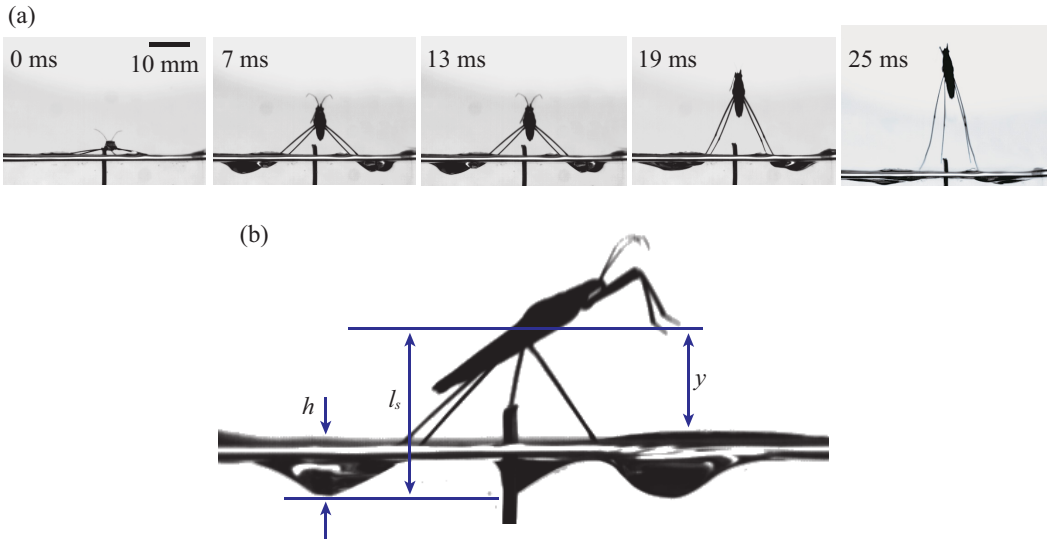

FIG. 1. (a) The front view of a water strider jumping off the water surface taken by a high-speed camera. (b) The side view of a water strider during its jump with length parameters used in the modeling. Adapted from Ref. [11].

body length. This amazing feat is closely related to their capabilities to effectively use the capillary force that the water surface provides [10].

The jumps of small arthropods are usually triggered by sudden attacks of predators, such as fish and backswimmers. As it is a matter of life and death, it is likely that their jumping is shaped by natural selection for optimal performance [11]. Therefore, understanding how they make such a dramatic motion for survival can shed light on the ultimate level of semiaquatic motility achievable through evolution. In addition, the physical analysis of the kinematics and dynamics of the natural creatures' water jumping can guide us to design and optimize microrobots that can jump off water surfaces at maximum efficiency.

In an attempt to emulate the jumping of a water strider on the water surface, Koh *et al.* [10] analyzed the trajectory of the strider legs and the resulting forces provided by the deforming water meniscus. Then a microrobot was developed which rotated its legs at a relatively low velocity with a force just below that required to break the water surface. Yang *et al.* [11] calculated the takeoff velocity of various species of medium-sized water striders by combining the force profile exerted on the legs and their rotational kinematics. The analysis led to the conclusion that the striders tune the stroke speed to nearly maximize the takeoff velocity. In addition to the strider, a mechanical version of a springtail was tested which required much fewer components than the robotic water strider [12].

In view of the recent achievements in elucidating the optimal strategy for jumping of water striders and currently growing interest in bioinspired soft robots [13], here we aim to provide a coherent review of the theories for jumping on water from the basics of how small objects float on water to the sophisticated behavior of water striders for improved efficiency. Furthermore, we need to answer the question of whether the theories can be applied to the jumping of other semiaquatic creatures. Therefore, in the following we start with reviewing the fundamental mechanics associated with floating of small objects at the air-water interface. Then we explain the theoretical framework to analyze and predict the jumping of a water strider off water surface. Further, we discuss the strategies adopted by the striders to enhance the takeoff velocity and consequently jumping height.

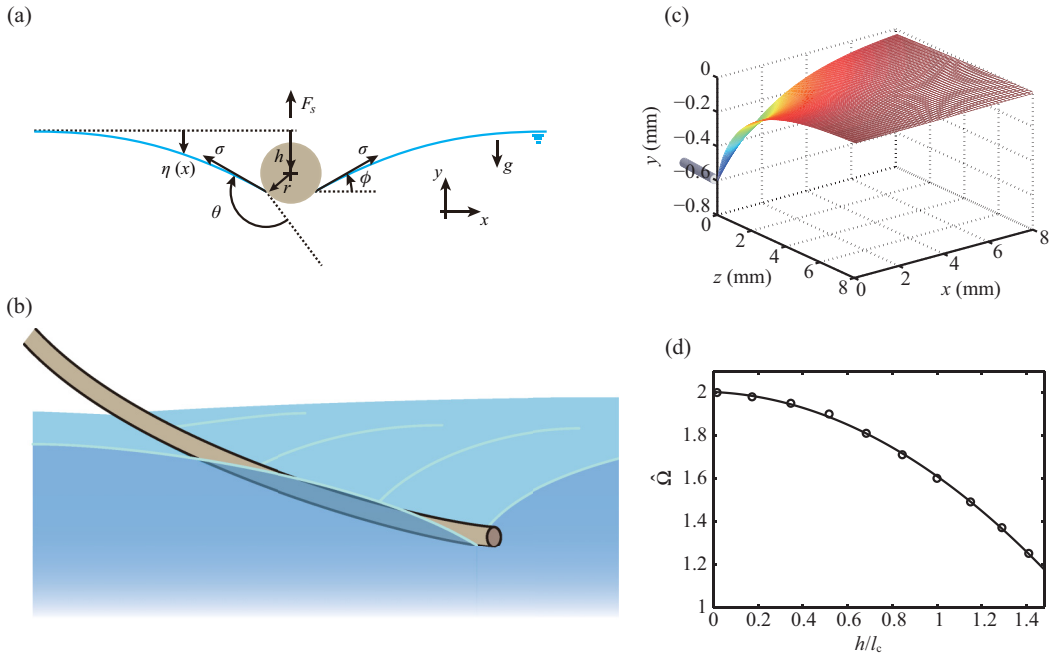

FIG. 2. (a) Forces acting on a cylinder floating on water. (b) The shape of a long flexible cylinder which is supported by the deformed interface. (c) The profile of meniscus extending from an end of a cylinder at depth $h = 0.6$ mm to the undisturbed free surface of water. The three-dimensional Laplace-Young equation was solved assuming that η at $z = 0$ is given by the two-dimensional Laplace-Young equation solved for the cylinder side. Only half the depressed surface (positive x) is shown for clarity. (d) The scaled volume, $\hat{\Omega} = \Omega/(l_c^2 h)$, displaced by the meniscus vs the scaled depth of the cylinder end, h/l_c. The circles are the computational results and the line is from the best-fitting formula.

Finally, we extend the theoretical approach to the jump of springtails, whose locomotory appendage is much shorter than the strider legs.

II. FORCE ON A FLOATING CYLINDER

To mathematically analyze the jumping of small arthropods on water, it is essential to understand the forces acting on a floating object as illustrated in Fig. 2. While a completely immersed body is under its own weight and hydrostatic pressure force in a static situation, the floating object experiences the additional force due to surface tension acting along the three phase (liquid-solid-gas) contact line in the direction tangential to the interface. Whether the surface tension will help the object to float or not, or the direction of the force (ϕ), depends on the contact angle θ, the relative elevation of the object, and the object shape. The restoring force on the floating body, a sum of the hydrostatic pressure force and the surface tension force, is equal to the weight of the liquid displaced by the solid object and the meniscus [14,15].

The length scale over which the meniscus profile decays is the capillary length $l_c = [\sigma/(\rho g)]^{1/2}$, with ρ and g being the water density and the gravitational acceleration, respectively. For an object with its characteristic length r being $r \ll l_c$, the restoring force is primarily due to surface tension. Here we are interested in the flotation of hydrophobic cylindrical objects because of their resemblance to locomotory appendages of water striders and springtails. For a cylinder whose cross section is shown in Fig. 2(a), the restoring force due to surface tension along its two sides, F_s', is given by $F_s' = 2\sigma l_w \sin\phi$, where l_w is the wetted length of the cylinder. By Keller's theorem [14], F_s' is equal to the weight displaced by the meniscus, which can be calculated by solving the two-dimensional

Laplace-Young equation:

$$\frac{\rho g}{\sigma}\eta = \frac{\eta_{xx}}{\left(1+\eta_{xx}^2\right)^{3/2}}, \tag{1}$$

where η is the deflection of the interface. It was shown that [16]

$$F_s' = 2\rho g l_c l_w h\left[1-\left(\frac{h}{2l_c}\right)^2\right]^{1/2}, \tag{2}$$

where h is the vertical downward distance of the cylinder from the undisturbed free surface. A cylinder with the radius $r \ll l_c$ sinks when h reaches $\sqrt{2}l_c$ corresponding to $\phi = \pi/2$, and thus $0 < h < \sqrt{2}l_c$ in Eq. (2).

When the cylinder is flexible due to its long and slender geometry, the bending of the cylinder along its length should be taken into account [17,18], as shown in Fig. 2(b). Although numerical computation is required to solve the beam equation with the meniscus shape given by the Laplace-Young equation at each position of the bent cylinder, we may simply modify Eq. (2) to express the force on the sides of a long but thin flexible cylinder as $F_s = CF_s'$ [11]. Here, the flexibility factor C depends on the scaled cylinder length $L = l_w/l_e$, where $l_e = (Bl_c/\sigma)^{1/4}$ is the modified elastocapillary length of the cylinder of radius r with the bending rigidity $B = \pi Er^4/4$: $C \approx (1+0.082L^{3.3})^{-1}$ for $L < 2$ and $C \approx (1.15L)^{-1}$ for $L > 2$.

In addition to the cylinder sides, the end tips of cylinders cause the interface deformation, contributing to the restoring force. To obtain the capillary force at the cylinder end, F_e, which is taken to be the weight of the water displaced by the meniscus formed by the tip of the cylinder [19], we first calculate the profile of the meniscus, $\eta(x,z)$, that extends from the depressed tip at $\eta = h$ to the undisturbed free surface. The interface shape is governed by the three-dimensional Laplace-Young equation [19]:

$$\frac{\rho g}{\sigma}\eta = \frac{\left(1+\eta_x^2\right)\eta_{zz} - 2\eta_x\eta_z\eta_{xz} + \left(1+\eta_z^2\right)\eta_{xx}}{\left(1+\eta_x^2+\eta_z^2\right)^{3/2}}. \tag{3}$$

It can be solved numerically, and the profile of the meniscus adjoining a tip of a thin superhydrophobic cylinder ($\theta = 167^\circ$, a typical value for superhydrophobic arthropods [20]) at $h = 0.6$ mm is shown in Fig. 2(c). The volume displaced by the meniscus $\Omega = \int_A \eta dA$ with A being the area in the xz plane, and the corresponding upward force $F_e = \rho g\Omega$.

We seek a simplified way to obtain F_e, which is primarily dependent on h for a thin superhydrophobic cylinder. When the water surface is depressed, the interface is deformed over a distance of the order of l_c. Therefore, the volume of water that is displaced by the meniscus extending from a point at the depth h as shown in Fig. 2(c) is scaled as $l_c^2 h$. We calculated the scaled volume $\hat{\Omega} = \Omega/(l_c^2 h)$ for varying $\hat{h} = h/l_c$ to find that $\hat{\Omega} \approx -0.35\hat{h}^2 - 0.04\hat{h} + 2.0$. See Fig. 2(d). Therefore, the upward force due to the cylinder end at depth h is simply given by $F_e = \rho g\hat{\Omega} l_c^2 h$. In particular, for $h \ll l_c$, $F_e \approx 2\rho g l_c^2 h$.

The total force acting on the floating cylinder $F = F_s + kF_e$ with $k = 2$ for a cylinder whose both ends touch the water surface and $k = 1$ for a cylinder with only one end depressing the water. The volume of the water displaced by the meniscus adjoining the cylinder side $\Omega_s \sim l_c l_w h$, while the volume displaced by the cylinder end $\Omega \sim l_c^2 h$. Hence, the relative importance of the capillary force acting on the cylinder end to that on the cylinder side is estimated as $\Omega/\Omega_s \sim l_c/l_w$. Therefore, the end force can be neglected when the wetted length of cylinder l_w is significantly greater than the capillary length of water, $l_c = 2.7$ mm.

III. ANALYSIS OF WATER STRIDER JUMPING

Figure 1(a) shows the snapshots of the front view of a water strider during its jump on water. A major goal of the theoretical analysis for this motion is to predict the temporal evolution of the body height as the strider rotates its middle and hind legs. In this section, we delineate the theoretical framework developed in Refs. [10,11] and present a result of predicting the body center height versus time. We first start by identifying the dominant force acting on the water strider legs. While the strider pushes the water surface down to create dimples, various forces are exerted on the insect's legs including the capillary force F, pressure force, buoyancy, added inertia, viscous drag, and the weight of the strider. With typical kinematic parameters for the medium-sized water strider species, the capillary force on the leg sides, $F_s \sim 2\sigma l_w$, turns out to be orders of magnitude greater than the other forces [10,11]. Also, we neglect the force acting on the end of the leg for its great length. Hence, the jump can be simplified as a surface-tension-dominant interaction of a long thin flexible cylinder with the water surface. Then the force acting on the four legs $F = 4F_s = 4CF_s'$ with F_s' given by Eq. (2).

The fact that the dimple depth gives the force acting on the legs with known properties of water and the leg allows us to calculate the body center height $y(t)$, t being time, with respect to the unperturbed free surface when the leg motion is prescribed. For the length symbols used in the modeling, see Fig. 1(b). The experimental measurements reveal that the leg rotation rate of the water striders can be approximated as a constant ω, leading us to write the downward linear velocity of the leg $v_s = \dot{l}_s = \omega(l_l - y_i)\sin(2\omega t)$, where the subscript s stands for stroke. Here, $l_s = y + h$ is the vertical distance from the body center to the tip of the leg, l_l is the entire length of the leg consisting of femur, tibia, and tarsus, and y_i is the initial height of the body center from the undisturbed free surface of water. For $l_s \approx y_i$ initially ($t = 0$), we obtain $l_s = \frac{1}{2}(l_l - y_i)[1 - \cos(2\omega t)] + y_i$.

We now describe the temporal evolution of h, which comes from Newton's second law of motion: $F = m\ddot{y}$ or $\ddot{h} = \ddot{l}_s - F[h(t),l_w(t)]/m$. Using Eq. (2), we obtain the second-order ordinary differential equation for h, which can be solved numerically. In the first (pushing) phase of the jump, $t = 0$ to $t_m = 13$ ms in Fig. 1(a), when the legs push the water surface down with a constant wetted length (the length of tibia plus tarsus, l_t), the initial conditions are such that $h(0) = \dot{h}(0) = 0$. In the second (closing) phase which starts upon the dimple depth reaching its maximum (h_m) at $t = t_m$, the legs slide on the water surface towards the body while gradually disengaging themselves from the water surface with a decrease in l_w. Thus, for the closing stage, we use $h(t_m) = h_m$ and $\dot{h}(t_m) = 0$ as the initial conditions and model the wetted length as $l_w = l_t(h/h_m)(\pi/2 - \omega t)/(\pi/2 - \omega t_m)$.

With l_s and h described as a function of time, we can find the temporal evolution of the body center height $y = l_s - h$. Also, the takeoff velocity of the water strider $\dot{y}(t_t)$ can be defined as the velocity at the moment when the end tips of the escaping legs reach zero depth, or $h(t_t) = 0$. In Fig. 3(a), we plot the theoretically predicted height of the body center versus time and find good agreement between theory and experiment.

The force acting on the four legs of a water strider until it disengages from the water surface is plotted versus time in Fig. 3(b). It is the area below the force-time curve that the strider needs to increase to maximize the takeoff velocity because $\dot{y}(t_t) = \int_0^{t_t} F dt/m$ by Newton's second law of motion. The maximum force that the strider leg can exert on the water surface is limited by the surface tension: 2σ per unit length. In this case, the dimple depth is also maximized to be $H = \sqrt{2}l_c$ [11]. In addition to the force value, the rate at which the force increases to its maximum should be limited for a few reasons. The rate corresponds to the descent speed of the legs, which in turn is determined by the leg rotation speed. The strength and agility of the strider muscles driving the leg rotation would be the natural limiting factor. Even when the capability of the muscle is sufficient, the leg will penetrate the water surface if it descends too fast before the body center rises. The penetration causes no splash due to the insignificant effect of inertia compared to capillary forces but dramatically reduces the water's reaction force. The total length of a water strider leg reaches approximately 22 mm, much longer than $H = 3.8$ mm, and thus merely pointing its legs downward without elevating its body would definitely cause the water penetration [see Fig. 4(a)]. It was reported in Ref. [11] that the

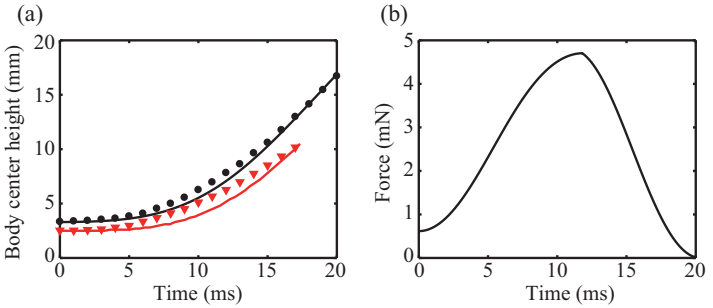

FIG. 3. (a) The height of body center of jumping water striders vs time. Circles and triangles correspond to the experimental results and lines correspond to the theoretical predictions. Black symbols correspond to the jump of a male *Aquarius paludum* with $m = 37$ mg, $r = 130$ μm, $l_l = 22.6$ mm, $l_w = 13$ mm, and $\omega = 60$ rad s^{-1}. Red symbols correspond to the jump of a male *Gerris paludum* with $m = 31$ mg, $r = 130$ μm, $l_l = 15.9$ mm, $l_w = 7.7$ mm, and $\omega = 77$ rad s^{-1}. (b) The force acting on a leg of a water strider vs time corresponding to the black symbols in panel (a).

medium-sized water strider species always tune their leg rotation speed so as to make the maximum dimple depth, $h(t_m)$, close to H. Such near-optimal rotation rates are approximately 60 and 77 rad s^{-1} for male *Aquarius paludum* and *Gerris paludum*, respectively, as used in Fig. 3.

With the maximum value and growth rate of the force being limited by the foregoing factors, it would be a natural strategy for the strider to prolong the interaction with water in order to increase the area under the force-time curve. To this end, the water strider rotates its legs, causing them to slide along the water surface, unlike most terrestrial animals that push down a fixed spot under their feet before jumping. In the pushing phase when the dimple depth grows with the descent of the strider leg, the effect of rotation is not prominent. But without rotation, the strider leg would no longer be in contact with water after the pushing phase because it would ascend too fast compared to the recovery rate of the dimple [see Fig. 4(b)]. The ascent speed or the takeoff speed, v, is of the order 1 m s^{-1} while the dimple recovery rate $U_r \sim l_c/t_r \sim 10^{-1}$ m s^{-1} as scaled using the dimple depth $\sim l_c$ and the characteristic time t_r for the capillary-gravity wave to travel the capillary length [21]. Through rotation, the legs can keep pressing the water surface during the closing phase and so exploit the capillary force that the water meniscus provides even after the dimple depth is maximized.

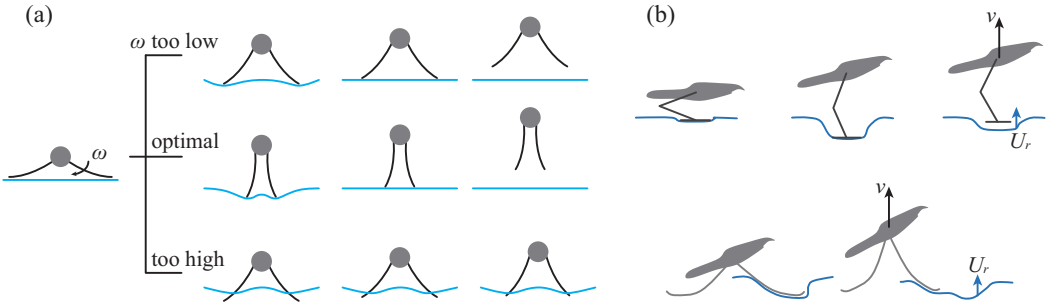

FIG. 4. (a) The effects of the leg rotation speed in the penetration of water surface. When the leg rotation rate ω is too high, the legs pierce the water surface, thereby failing to use the capillary force. (b) The role of leg rotation in prolonging the interaction between the leg and water surface. In the upper case where the leg pushes down the water surface without rotation, the leg is disengaged from the water surface too early. In the lower case where the leg rotates, the interaction time of leg and water surface increases.

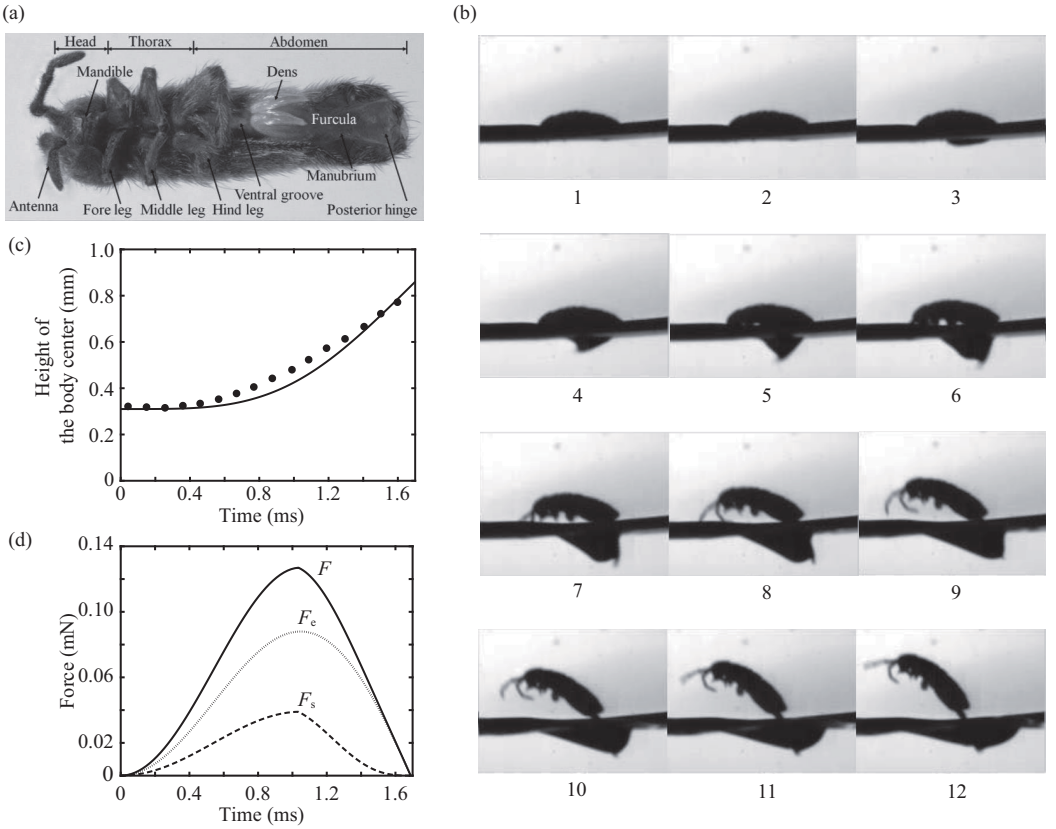

FIG. 5. (a) Micrograph of a springtail with the body length of 1.7 mm. (b) Time series of jumping of the springtail on the water surface. The time interval between the adjacent images is 0.2 ms. (c) The height of the body center vs time. The circles correspond to the measurement result of Ref. [5] and the line is our theoretical prediction. (d) The temporal evolution of the total capillary force F consisting of the forces on the side (F_s) and the end (F_e) of the furcula. Panels (a) and (b) reprinted with permission from Sudo *et al.* [5], copyright 2015 by the Japanese Society for Experimental Mechanics.

IV. ANALYSIS OF SPRINGTAIL JUMPING

Springtails are tiny hexapods living on land and water that have a body length of only a few millimeters. They have an abdominal appendage called furcula, which is folded beneath the body but released to snap against the substrate (either solid or water) when threatened, launching the animal into air. Figure 5(a) shows the micrograph of a springtail, *Podura aquatica*, whose jumping was filmed with a high-speed camera [5]. The furcula is forked at the end of the cylindrical basal part (manubrium). As shown in Fig. 5(b), a dimple is formed on the water surface as the furcula rotates, a similar process to what is observed in the jump of a water strider.

The forces acting on the furcula include the capillary force $F \sim 2\sigma l_w$, pressure force $F_p \sim \rho U^2 r l_w$, buoyancy $F_b \sim \rho g r \tilde{h} l_w$, added inertia $F_a \sim \rho r^2 l_w U^2/\tilde{h}$, viscous force $F_v \sim \mu r l_w U/l_c$, and the weight of the springtail $F_w \sim mg$. Here r is the characteristic radius of the furcula taken to be similar to that of the manubrium, 85 μm in Fig. 5(a). U is the rate of vertical growth of the dimple ($\sim$0.1 m s^{-1}), μ is the viscosity of water, and m is the mass of the springtail taken to be 0.15 mg as an average value [22,23]. The wetted length l_w corresponds to the length of the furcula, measured to be 1.1 mm from the image of the extended furcula in Ref. [5]. The comparison of the magnitude of

the aforementioned forces reveals that the capillary force dominates the other forces in the jump of springtails, just as for water striders.

The growth of the dimple volume corresponds to the increase of the upward capillary force, which lifts the body center. Therefore, we again write the height of the body center $y(t) = l_s(t) - h(t)$, where l_s is the vertical distance from the body center to the tip of the furcula. We use the average angular velocity of the furcula measured in Fig. 5(b), $\omega = 1300$ rad s^{-1}, to give $l_s = \frac{1}{2}(l_f - y_i)[1 - \cos(2\omega t)] + y_i$, where l_f is the furcula length. We take the wetted length $l_w = l_f$ from the beginning to the moment when the dimple depth is maximized ($t = t_m$). For $t > t_m$, the wetted length reduces with time as the furcula is disengaged from the water surface. It is modeled by $l_w = l_f(h/h_m)(\theta_m - \omega t)/(\theta_m - \omega t_m)$, where the maximum stroke angle $\theta_m = 2.22$ rad is greater than $\pi/2$, the maximum value for the water strider. To obtain $h(t)$, we use Newton's second law of motion: $\ddot{h} = \ddot{l}_s - F/m$ with F determined in the following.

For the water striders having a wetted length significantly greater than l_c, the capillary force acting along the sides of the leg is dominant, allowing us to estimate $F \approx F_s$. However, in evaluating the capillary force on a short cylinder, like the furcula of the springtail, the force acting at the end cannot be ignored for $l_w < l_c$. Then we write the total force that supports the appendage as $F = F_s + F_e$. Although numerical computations of the two- and three-dimensional Laplace-Young equations are necessary to rigorously evaluate F_s and F_e, respectively, we may use the simplified expressions for the forces that fit the numerical results, $F_s = 4CF_s'$ and $F_e = \rho g \hat{\Omega} l_c^2 h$, as provided above.

Now we solve the differential equation for h with a known expression of F with respect to h, which finally gives $y(t)$ in the same manner as for the water strider. Figure 5(c) shows that the theoretically predicted height of the springtail's body center versus time agrees well with the measurement result, demonstrating that the theoretical framework developed for the water strider can be applied to other semiaquatic jumping animals as well. Figure 5(d) compares the magnitudes of F_s and F_e in the jumping of the springtail, to reveal that F_e is greater than F_s, taking up to 69% of the entire force. Unlike the water striders, which have legs longer than the maximum dimple depth that the water surface allows, H, and consequently need to control the leg stroke speed not to break the water surface, the springtails have no danger of piercing the water surface for their short furcula. Thus, the snapping speed of the furcula of a given length is the key parameter that determines the takeoff velocity and the jumping height.

V. CONCLUSIONS

It is an exquisite feat of nature that small semiaquatic arthropods like water striders and springtails can jump off the water surface to a height several times their body length without sinking. Building upon the previous works that have delved into the secret of successful jumping on water [10] and the optimized motion strategy to maximize the chance to escape from danger [11], we have delineated the mathematical theory to predict the body height as a function of time with given information of leg morphology, properties, and kinematics. While the foregoing analyses of floating and jumping of semiaquatic insects [10,11,17] considered the capillary force acting along the sides of the cylindrical leg only, we have newly added the contribution of the water weight displaced by the meniscus adjoining the leg tip. The new addition, which was unnecessary for the jumping of water striders with relatively long legs, has allowed us to correctly predict the jumping of springtails with a relatively short locomotory appendage.

A number of exciting problems in the mechanical analysis of water jumping await to be explored in the future, as listed partially in the following. First, the ability of the water strider to control its jumping direction or angle is of interest. In our experiments, the jump trajectories of striders deviated from the vertical in some cases, which were controlled by the delicate motion of the middle and hind legs. How the insect effectively uses the capillary force to produce the reaction in the horizontal direction may open up a new pathway to enable a novel locomotion scheme on water. Second, the role of microscale hairs covering the legs of water striders at a slanted angle [1] in the jumping performance needs to be investigated. The asymmetric friction with water due to hair angle might

contribute to the enhancement of efficiency and the reduction of chance of water penetration [24]. Third, the optimal design and motion principle of the furcula of the springtail is unknown. Since it does not penetrate the water surface, the motion strategy discovered for the water strider seems irrelevant. The forked end region termed "dens" in Fig. 5(a) is rather smooth without hairs, and thus it is speculated to be relatively hydrophilic and so responsible for the partial water penetration evident in Fig. 5(b). The smooth part may be used in anchoring the body on water [1]. Consideration of the diverse functions of the appendage will result in the full physical understanding of its design.

Mathematical approaches to analyzing the locomotory behavior of biological creatures have played a pivotal role in elucidating their optimal design principle to survive and prosper through a long history of natural selection [25,26]. The present work carries on the theoretical endeavors to mechanically analyze the horizontal [2,4,27] and vertical [10,11] motion of semiaquatic arthropods. The physical findings have helped and will continue to inspire biologists to understand the evolutionary pressure that shaped the anatomical, morphological, and kinematic traits of each species living on water. Furthermore, the fundamental design principles and motion strategies learned from the semiaquatic arthropods can serve as a guideline to develop robots that can exhibit superior maneuverability on water with a maximized efficiency.

ACKNOWLEDGMENTS

We thank Prof. L. Mahadevan, Prof. Haecheon Choi, and Prof. Kyu-Jin Cho for helpful discussion. This work was supported by National Research Foundation of Korea (Grants No. 2016901290, No. 2016913167, and No. 2016R1D1A1B03934340) and Disaster and Safety Management Institute, Korea Coast Guard (Grant No. KCG-01-2017-02) via SNU-IAMD.

[1] J. W. M. Bush, D. L. Hu, and M. Prakash, The integument of water-walking arthropods: Form and function, Adv. Insect Phys. **34**, 112 (2008).
[2] J. W. M. Bush and D. L. Hu, Walking on water: Biolocomotion at the interface, Annu. Rev. Fluid Mech. **38**, 339 (2006).
[3] D. L. Hu and J. W. M. Bush, Meniscus-climbing insects, Nature (London) **437**, 733 (2005).
[4] D. L. Hu and J. W. M. Bush, The hydrodynamics of water-walking arthropods, J. Fluid Mech. **644**, 5 (2010).
[5] S. Sudo, T. Kainuma, T. Yano, A. Shirai, and T. Hayase, Jumps of water springtail and morphology of the jumping organ, J. JSEM **15**, s117 (2015).
[6] R. J. Waggett and E. J. Buskey, Calanoid copepod escape behavior in response to a visual predator, Mar. Biol. **150**, 599 (2007).
[7] S. J. Kim, J. Hasanyan, B. J. Gemmell, S. Lee, and S. Jung, Dynamic criteria of plankton jumping out of water, J. R. Soc., Interface **12**, 20150582 (2015).
[8] R. P. Wilson, M.-P. T. Wilson, and E. C. Nöldeke, Pre-dive leaps in diving birds; Why do kickers sometimes jump, Mar. Ornithol. **20**, 7 (1992).
[9] D. Au and D. Weihs, At high speeds dolphins save energy by leaping, Nature (London) **284**, 548 (1980).
[10] J.-S. Koh, E. Yang, G.-P. Jung, S.-P. Jung, J. H. Son, S.-I. Lee, P. G. Jablonski, R. J. Wood, H.-Y. Kim, and K.-J. Cho, Jumping on water: Surface tension-dominated jumping of water striders and robotic insects, Science **349**, 517 (2015).
[11] E. Yang, J. H. Son, S. Lee, P. G. Jablonski, and H.-Y. Kim, Water striders adjust leg movement speed to optimize takeoff velocity for their morphology, Nat. Commun. **7**, 13698 (2016).
[12] D. L. Hu, M. Prakash, B. Chan, and J. W. M. Bush, Water-walking devices, Exp. Fluids **43**, 769 (2007).
[13] D. Rus and M. T. Tolley, Design, fabrication and control of soft robots, Nature (London) **521**, 467 (2015).
[14] J. B. Keller, Surface tension force on a partly submerged body, Phys. Fluids **10**, 3009 (1998).

[15] D. Vella, Floating versus sinking, Annu. Rev. Fluid Mech. **47**, 115 (2015).
[16] D. Vella, D.-G. Lee, and H.-Y. Kim, The load supported by small floating objects, Langmuir **22**, 5979 (2006).
[17] D. Vella, Floating objects with finite resistance to bending, Langmuir **24**, 8701 (2008).
[18] K. J. Park and H.-Y. Kim, Bending of floating flexible legs, J. Fluid Mech. **610**, 381 (2008).
[19] D.-G. Lee and H.-Y. Kim, The role of superhydrophobicity in the adhesion of a floating cylinder, J. Fluid Mech. **624**, 23 (2009).
[20] X. Gao and L. Jiang, Water-repellent legs of water striders, Nature (London) **432**, 36 (2004).
[21] D. Vella, D.-G. Lee, and H.-Y. Kim, Sinking of a horizontal cylinder, Langmuir **22**, 2972 (2006).
[22] H. A. Verhoef and J. Witteveen, Water balance collembola and its relation to habitat selection: Cuticular water loss and water uptake, J. Insect Physiol. **26**, 201 (1980).
[23] J. O. Wolff, A. L. Schönhofer, C. F. Schaber, and S. N. Gorb, Gluing the "unwettable": Soil-dwelling harvestmen use viscoelastic fluids for capturing springtails, J. Exp. Biol. **217**, 3535 (2014).
[24] M. Prakash and J. W. M. Bush, Interfacial propulsion by directional adhesion, Int. J. Nonlinear Mech. **46**, 607 (2011).
[25] S. Vogel, *Life in Moving Fluids: The Physical Biology of Flow*, 2nd ed. (Princeton University Press, Princeton, NJ, 1996).
[26] J. M. Skotheim and L. Mahadevan, Physical limits and design principles for plant and fungal movements, Science **308**, 1308 (2005).
[27] D. L. Hu, B. Chan, and J. W. M. Bush, The hydrodynamics of water strider locomotion, Nature (London) **424**, 663 (2003).